Journal of Renewable Energies

Revue des Energies Renouvelables

journal home page: https://revue.cder.dz/index.php/rer

Research paper

Integrated Square On-Chip Inductor for Photovoltaic Converter Applications

Mokhtaria Derkaoui [a,*], **Yamina Benhadda** [b]

[a] *LARATIC Laboratory, National Higher School of Telecommunications & ICT of Oran, Algeria*

[b] *LEPA Laboratory, University of Sciences and Technology of Oran, Algeria*.

ARTICLE INFO

Article history:
Received March 22, 2024
Accepted April 22, 2024

Keywords:
DC-DC Buck Converter
Inductor
Integration
On-Chip
PV

ABSTRACT

The research of this paper concerns the study of an integrated square on-chip inductor in a DC-DC Buck converter connected to a photovoltaic module. The topology of the inductor is chosen for its ability to provide improved performance and high inductance value. The paper presents the integrated inductor geometrical and electrical dimensioning. The equivalent electrical circuit of an on-chip inductor with different added layers is described. The finite elements method is used to illustrate the current density and temperature distribution in the on-chip spiral inductor. The simulation of the DC-DC Buck converter with a PV panel is validated using the integrated inductor to show its performance. The study combines theoretical analysis, modeling, and simulation techniques to evaluate the performance and effectiveness of the square on-chip inductor topology. The results obtained provide valuable insights into the design and operation of the integrated inductor-based PV system.

1. INTRODUCTION

Solar energy is an important renewable energy source that is environmentally friendly and its applications in photovoltaic (PV) systems are increasing [1-2]. The electric power generated by a photovoltaic system is influenced by solar radiation and temperature variations [3-4]. The maximum power produced by the photovoltaic (PV) module is delivered to the load by adjusting the voltage through a DC-DC converter [5]. DC-DC converters play a crucial role in these systems by simplifying the conversion and distribution of power [6-7]. This miniaturization of converters has pushed toward the development of distributed architectures and embedded systems for on-chip systems containing several components [8-9]. Therefore, the integration of the passive components of these converters becomes an inevitable solution to reduce sizes and costs [10-11]. On-chip integrated planar inductors

* *Corresponding author, E-mail address: mokhtaria.derkaoui@ensttic.dz*

ISSN: 1112-2242 / EISSN: 2716-8247

remove several inconveniences, in recent years [12-13]. This paper aims to address the challenges in PV systems containing a DC-DC converter with an integrated on-chip inductor. We propose a comprehensive study on the topology of the square spiral planar inductor integrated into a DC-DC Buck converter, which offers improved performance and a high inductance value. The model presented in this study includes geometric and electric characteristics to develop analytical equations for the inductor topology. Besides, we focus on implementing a PV system for the DC-DC converter, which integrates the proposed square inductor. This control strategy aims to operate the PV panel at its maximum power point, optimizing the overall energy conversion efficiency of the system. The performance of the integrated on-chip inductor in the converter is validated using specialized software. The simulations allow us to evaluate the effectiveness and efficiency of the designed integrated inductor in the DC-DC Buck converter and its application in photovoltaic systems.

2. METHODOLOGY AND MODELLING OF DC-DC BUCK CONVERTER

The DC-DC Buck converter can decrease the input voltage (Fig.1). It is frequently used in photovoltaic applications due to its high efficiency and easy implementation. To enhance the efficiency of PV systems, DC-DC converters are employed between the solar panels and the loads [6]. These converters enable the adaptation of input resistance to the output resistor, thus optimizing power transfer. The block diagram of a typical photovoltaic system is illustrated in Fig.2.

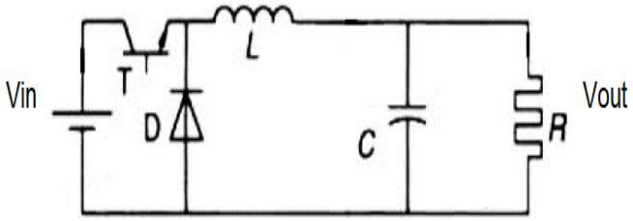

Fig 1. Conventional DC-DC Buck Converter

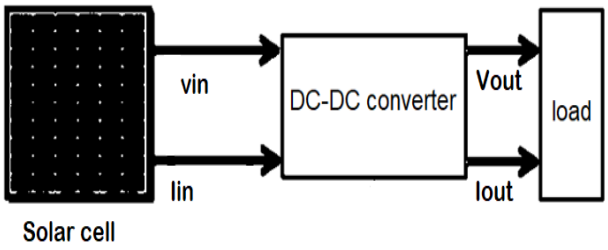

Fig.2. Block diagram of Photovoltaic system

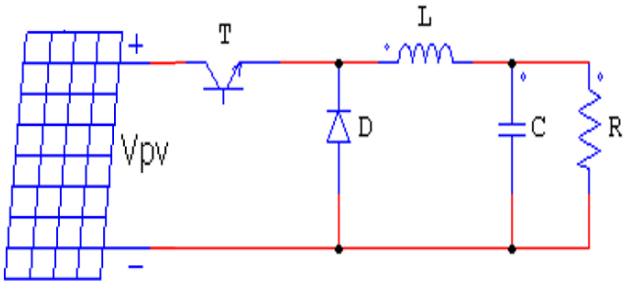

Fig.3. PV panel integrated with DC-DC Buck converter

As shown in Fig.3, the DC-DC Buck converter consists of a PV voltage source, inductor L, capacitor C, load resistor R, and also both transistors and diodes operating as switches.

The objective of this study is to reduce the size of the converter and preserve its performance. The main problem is to reduce the size of the inductor. The dimensions of the on-chip inductor to be integrated into the DC-DC Buck converter will be determined by the characteristics indicated in Table 1.

Table 1. Converter specifications

Input voltage V_{in}	5 V
Output voltage V_{out}	2.5 V
Output power P_{out}	1 W
Operating frequency f	500 kHz

The global model of a PV cell includes a diode connected in parallel with a current source, in addition to series and parallel resistances (Fig.4) [3]. The technical characteristics of the PV panel are determined in Table 2.

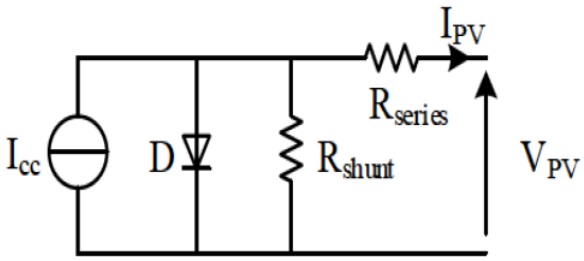

Fig.4. Equivalent circuit of PV cell

Table 2. PV panel technical characteristics

Maximum working voltage	12 V
Maximum current	0,5 A
Maximum power	3 W
Minimum working voltage	1 V
Maximum power tolerance	15%
Working temperature	-45°C to +85 °C

The average output current is given by (1).

$$I_{out} = \frac{P_{out}}{V_{out}} \tag{1}$$

The peak amplitude of the current flowing through the inductor is given by (2).

$$(\Delta I_L) = I_{Lmax} - I_{Lmin} = \frac{V_{in}}{4 \cdot L \cdot f} \tag{2}$$

The relation between the current supplied by the cell I_{PV} and the voltage across the cell V_{PV} is given by (3) [2].

$$I_{PV} = I_{cc} - I_{sat}\left[\exp\left(\frac{q \cdot V_{PV}}{n \cdot K \cdot T_c} + I \cdot R_{series}\right) - 1\right] \tag{3}$$

I_{sat}: junction saturation current

K: Boltzmann constant

T_c: cell temperature

q : electron charge

n: non-ideality factor of the junction

3. DIMENSIONING OF THE INTEGRATED ON-CHIP INDUCTOR

The integrated planar inductor consists of a square spiral coil in copper (Cu). The planar spiral coil is superimposed on the NiZn ferrite layer and isolated from there by the SiO_2 silicon dioxide layer. All these different layers with different materials are superimposed on the silicon layer (Si), which serves as a substrate (Fig.5).

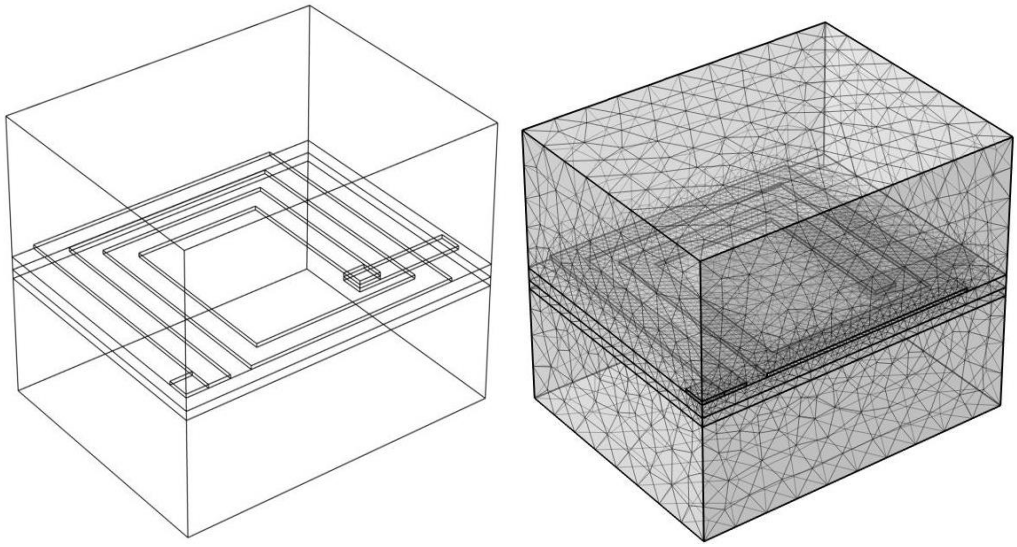

(a) (b)

Fig.5. (a) Square on-chip inductor 3D view, (b) Mesh

The required NiZn ferrite volume for the energy storage is given by (4).

$$V_{indu} = \frac{W_{indu}}{W_{vmax}} \tag{4}$$

W_{indu} and W_{vmax} represent the total magnetic stored energy (5) and the maximum volume density of energy (6) [12].

$$W_{indu} = \frac{1}{2} \cdot L \cdot I_{out}^2 \tag{5}$$

$$W_{vmax} = \frac{B_{max}^2}{2 \cdot \mu_0 \cdot \mu_{rNiZn}} \tag{6}$$

B_{max}= 0.3 T

μ_{rNiZn}= 1500

Therefore, 9.8125 mm^3 of NiZn is necessary to store 1 µJ of energy in the inductor.

The integrated square planar spiral inductor is characterized by geometrical parameters (Table 3), the angles are limited to multiples of 45 degrees.

Table 3. Geometrical parameter values

Geometrical parameters	Values
Outer diameter d_{out}	3 mm
Inner diameter d_{in}	1.2 mm
Turns number n	2
Coil thickness t	34 µm
Coil width w	25 µm
Coil total length l_t	9 mm
Coil spacing s	2.17 µm

The equivalent electrical circuit extracted from Fig.5 determines the electrical behavior of the integrated planar inductor. Different structures have been proposed for the integrated inductors, however, the most successful design is illustrated in Fig.6, which has been widely studied [12-14]. The circuit contains different electrical parameters that define each material layer. They are calculated by (7-13) and the different values are grouped in Table 5.

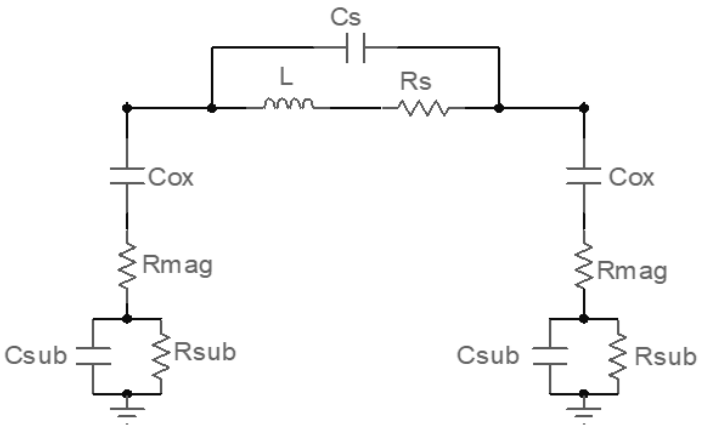

Fig.6. Lumped elements equivalent electrical circuit

The inductance value is calculated using Wheeler method (7) [10].

$$L = k_1 \cdot \mu_0 \cdot \frac{n^2 \cdot \left(\frac{d_{out}+d_{in}}{2}\right)}{1+k_2 \cdot \left(\frac{d_{out}-d_{in}}{d_{out}+d_{in}}\right)} \tag{7}$$

k_1 and k_2 represent the coefficients used in Wheeler expression for different coil topologies

Table 4. k_1 and k_2 coefficients values

Form	k_1	k_2
Square	2.34	2.75
Hexagonal	2.33	3.82
Octagonal	2.25	3.55

$$Rs = \rho_{cu} \cdot \frac{lt}{w \cdot t} \tag{8}$$

$$R_{mag} = 2 \cdot \rho_{NiZn} \cdot \frac{t_{mag}}{w \cdot lt} \tag{9}$$

$$R_{sub} = 2 \cdot \rho_{Si} \cdot \frac{t_{Sub}}{w \cdot lt} \tag{10}$$

$$C_{sub} = \frac{1}{2} \cdot \varepsilon_0 \cdot \varepsilon_{rSi} \cdot \frac{w \cdot lt}{t_{sub}} \tag{11}$$

$$C_{ox} = \frac{1}{2} \cdot \varepsilon_0 \varepsilon_{rSiO2} \cdot \frac{w \cdot lt}{t_{ox}} \quad (12)$$

$$C_s = \frac{1}{2} \cdot \varepsilon_0 \varepsilon_{rair} \cdot \frac{t \cdot lt}{s} \quad (13)$$

Where t_{mag} is the ferrite thickness, t_{sub} is the substrate thickness and t_{ox} is the oxide layer thickness.

$\rho_{NiZn} = 1000\ \Omega \cdot m$

$\rho_{Cu} = 1.7 \cdot 10^{-8}\ \Omega \cdot m$

$\rho_{Si} = 18.5\ \Omega \cdot m$

$\varepsilon_{rSi} = 11.8$

Table 5. Electrical parameters values

Electrical parameters	Values
Inductance L	3.125 µH
Serial resistance Rs	0.75 Ω
Magnetic resistance R_{mag}	2.8 MΩ
Substrate resistance R_{sub}	2.86 Ω
Substrate capacitance C_{sub}	17.43 pF
Oxide capacitance C_{ox}	11.149 Pf
Coil capacitance Cs	0.338 pF

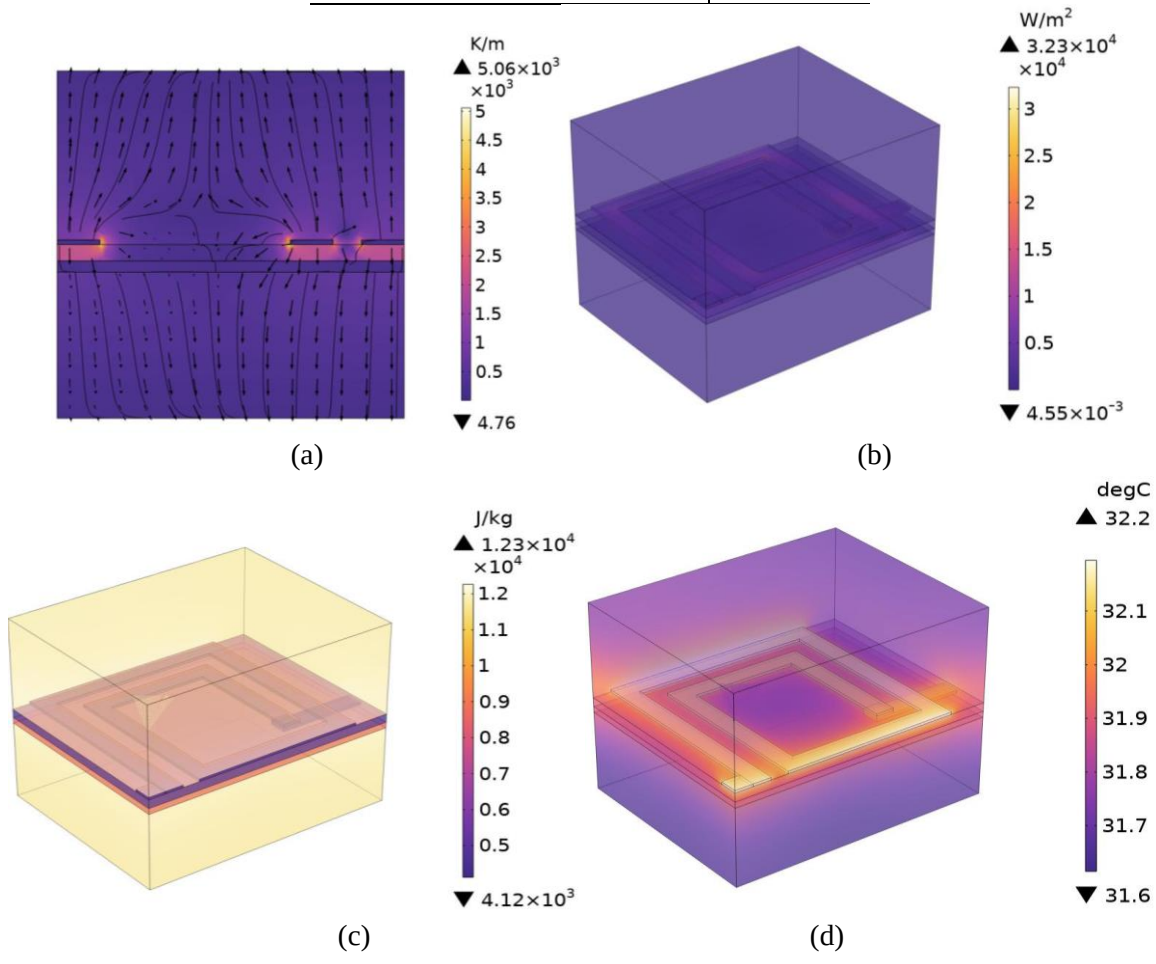

Fig.7. (a) Temperature gradient, (b) Total heat flow (c) Enthalpy, (d) Temperature

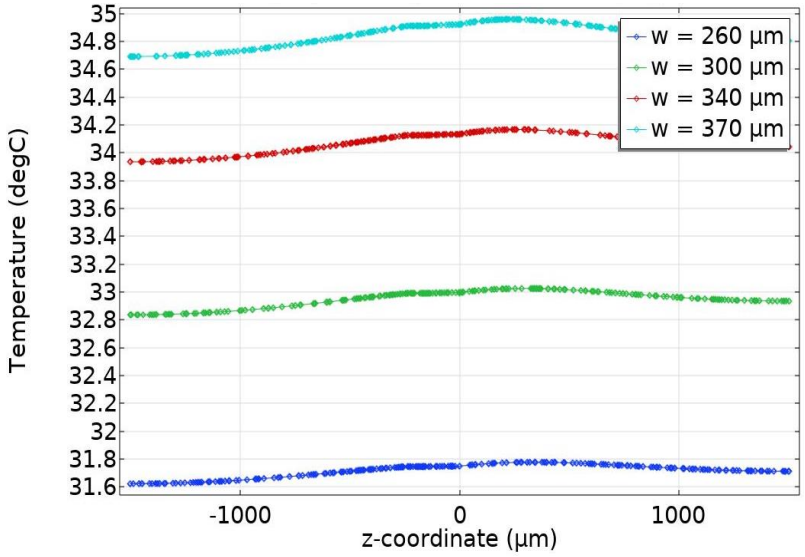

(a)

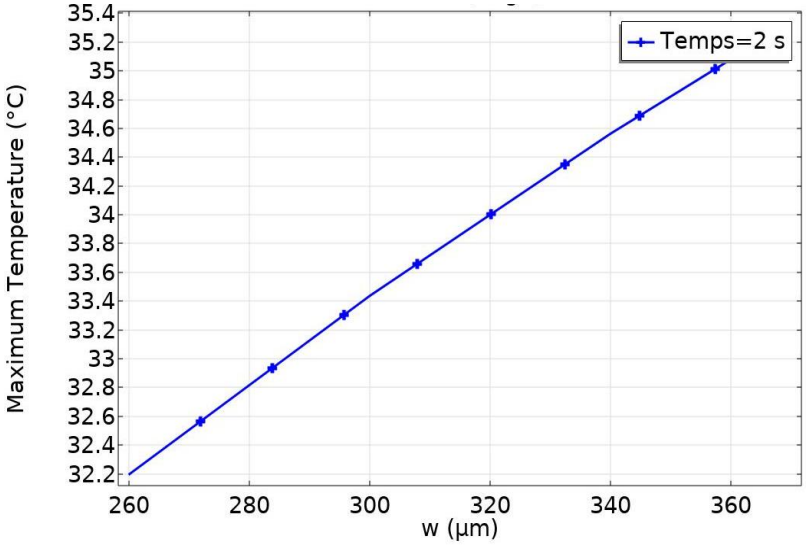

(b)

Fig.8. (a) temperature distribution in the inductor for different widths, (b) Maximum temperature versus width

The simulation was done by finite element method software to observe temperature gradient, total heat flow, enthalpy, and temperature distribution in the inductor at the operating frequency of 500 kHz (Fig.7). Besides, the impact of the width on temperature.

4. SIMULATION OF DC-DC BUCK CONVERTER FOR PHOTOVOLTAIC APPLICATIONS

The PV panel allows to convert the thermal energy into electricity. Fig.9 shows the circuit diagram of the DC-DC Buck converter containing the PV panel and the equivalent electrical circuit of the integrated on-chip inductor. This structure allows the efficient conversion of the output variable from the photovoltaic cell to a chosen output voltage and current level.

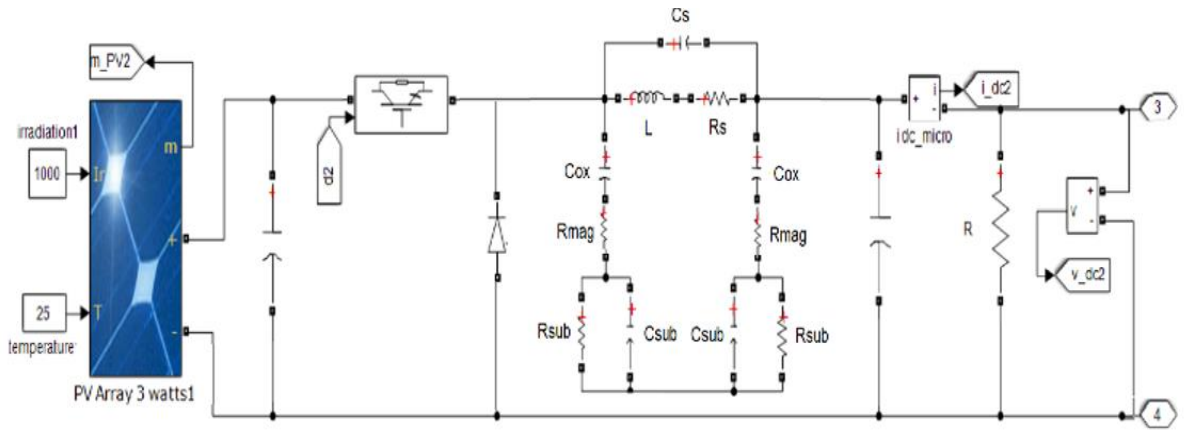

Fig.9. Photovoltaic system using DC-DC Buck converter with integrated on-chip inductor

Simulated results of the DC-DC Buck converter at a switching frequency of 500 kHz are presented in Fig.10. We notice that the maximum photovoltaic current achieves 0.8 A and the power is about 2.9 Watt for a voltage of 3 V. These results show that the integrated on-chip planar inductor works well. Hence, we can confirm that the geometrical and electrical dimensions are well defined.

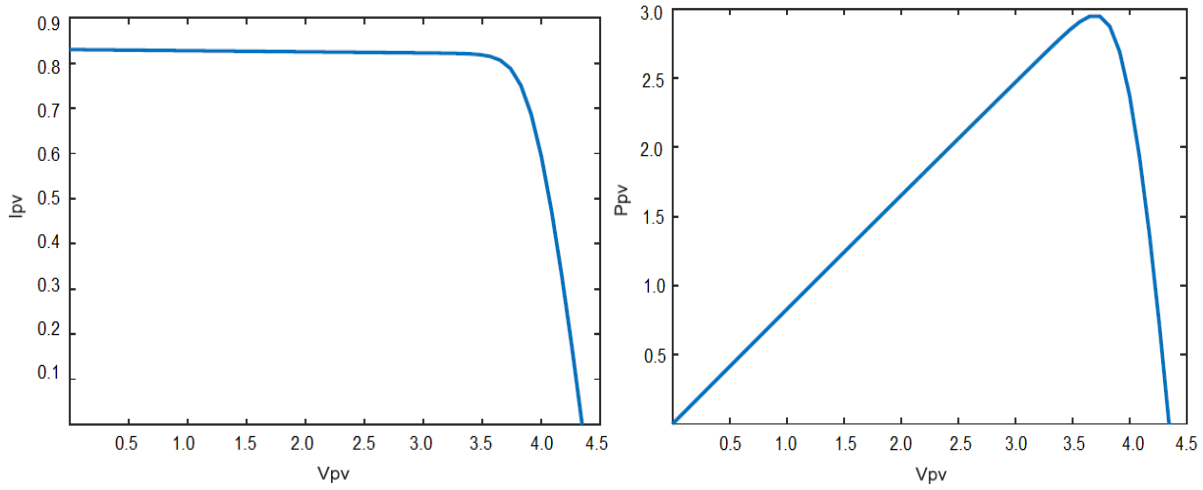

(a) (b)

Fig. 10. (a) I-V and (b) P-V Characteristics of Solar Cell

5. CONCLUSION

In this paper, we have presented the dimensioning, modeling, and simulation of the square on-chip planar inductor integrated into the DC-DC Buck converter used for the PV system. Simulations were established to evaluate the photovoltaic panel behavior. The simulations were conducted under a temperature of 25°C and constant irradiation of 1 kW/m². We have extracted the geometrical and electrical parameters of the integrated square planar inductor based on the specifications of the DC-DC Buck converter. By using a software simulation, we have extracted converter output current and power waveforms. The results obtained in this work serve as a valuable reference for the inductor integration into photovoltaic applications. The square on-chip planar inductor was found appropriate for operating the DC-DC Buck converter combined with the photovoltaic generator. We conclude that the results of dimensioning in this work are interesting indeed.

REFERENCES

Aldoumani, M.; Yuce, B.; Zhu, D. Using the Variable Geometry in a Planar Inductor for an Optimised Performance. Electronics 2021, 10, 721.

Benhadda, Y., Derkaoui, M., Mendaz, K., Kharbouch, H., Spiteri, P. "Design for Integrated Planar Spiral Inductor for MEMS", Periodica Polytechnica Electrical Engineering and Computer Science, (2023).

Derkaoui M, Benhadda Y, Hamid A, Temmar A. (2021) Design and modeling of square planar inductor and transformer in monolithic technology for RF systems. J Electr Eng Technol 16:1481–1493.

Derkaoui, M.; Benhadda Y.; Chaabene G.; Spiteri P.; "On-Chip GaN Planar Transformer Design for Highly Integrated RF Systems", Journal of Circuits, Systems and Computers, Vol. 32, No. 09, 2350149 (2023).

G. Pratapsinh Parmar and D. Urvashi Patel, "A Review on DC-DC converters for Photovoltaic system," IJIREEICE, vol. 3, no. 12, pp. 143– 146, Dec. 2015.

J. J. Khanam, S. Y. Foo, Modeling of a photovoltaic array in MATLAB Simulink and maximum power point tracking using neural network, Electrical & Electronic Technology Open Access Journal, vol. 2, no. 2, 2018.

K. V. G. Raghavendra, *et al*, "A Comprehensive Review of DC-DC Converter Topologies and Modulation Strategies with Recent Advances in Solar Photovoltaic Systems," Electronics, vol. 31, n. 9, p 1- 41, 2020.

M. H. Bechir, *et al*, "Planar inductor equivalent circuit model taking into account magnetic permeability, loss tangent, skin and proximity effects versus frequency," Analog integrated circuits and signal processing, vol.88, n.1, p 105–113, 2016.

M. R. Benzidane, *et al*, "Miniaturization, and Optimization of a DC–DC Boost Converter for Photovoltaic Application by Designing an Integrated Dual-Layer Inductor Model," Transactions on Electrical and Electronic Materials, vol. 23, p 462–475, 2022.

N. Belhaouas, M.S. Ait Cheikh, A. Malek, C. Larbes, Matlab-Simulink of photovoltaic system based on a two-diode model simulator with shaded solar cells, Revue des Energies Renouvelables, vol. 16, no.1, pp 65 – 73, 2013.

O. Ibrahim, N. Z. Yahaya, Matlab/Simulink Model of Solar PV Array with Perturb and Observe MPPT for Maximising PV Array Efficiency, 2015 IEEE.

R. Gladwin Antony, *et al*, "Design of Solar Charging Case for Mobile Phones," Journal of Physics: Conference Series (International Conference on Physics and Energy), vol. 2040, 2021.

S. Saravanan, N.R. Babu, "A modified high step-up non-isolated DC–DC converter for PV application," Journal of Applied Research and Technology, vol. 15, n.3, p 242–247, 2017.

Zaghba, A. Borni, A. Bouchakour, N. Terki, Buck-boost converter system modelling and incremental inductance algorithm for photovoltaic system via Matlab/Simulink, Revue des Energies Renouvelables SIENR'14 Ghardaïa (2014), pp 63 – 70.